

Motion and Dissolution of Drops of Sparingly Soluble Alcohols on Water

C. M. Bates, F. Stevens, S. C. Langford, and J. T. Dickinson*

Physics Department, Washington State University, Pullman, Washington 99164-2814

Received July 5, 2007. Revised Manuscript Received April 30, 2008

The dissolution of liquids with low mutual solubility is typically slow. However, drops of sparingly soluble, low-density, low-surface-tension liquids often dissolve rapidly on water due to surface tension instabilities and gradients. We report observations of the motion and dissolution of drops of aliphatic alcohols of a wide range of alkyl chain lengths as they dissolve in water. The alcohol drops are rendered visible by adding small amounts of iodine or other dyes. These drops display dewetting instabilities, fragmentation, fingering, and oscillation. As the length of the alcohol carbon chain increases from $n = 4$ to $n = 9$, dissolution slows dramatically. The roles of alcohol solubility and water surface area in promoting rapid dissolution are discussed.

Introduction

Drops of pure, immiscible liquids on water typically form compact lenses. (Most liquids that form thicker films on water, such as motor oil, are mixtures.) However, some pure liquids show more complex behavior, forming lenses that pulse, scoot about, and fragment into smaller lenses. These complex motions are common in liquids which are slightly soluble in water and reflect dewetting instabilities and surface tension inhomogeneities that develop in the early stages of dissolution.

In this work, we examine the behavior of small drops (typically 10 μL) of alcohols with modest chain lengths ($4 \leq n < 9$, where n is the number of carbon atoms), which show vigorous activity on pure water.^{1–5} This activity is often similar to the “camphor dance”^{3,6,7} displayed by pieces of camphor where they spin and dart across a water surface.

For many of the alcohols in this work, dewetting instabilities play an important role in the early stages of drop evolution. The instability of the initial drop configuration is due to the high surface tension of pure water, which exceeds the sum of the alcohol surface tension and the alcohol/water interfacial tension.^{8,9} Initially quiescent lenses of room-temperature 1-alcohols with $n = 5–7$ soon develop particularly unstable configurations, where a thickened rim surrounds a thin central region. These lenses often collapse to produce a crescent- or boomerang-shaped lens that subsequently rebounds and fragments. In the case of 1-heptanol, we show that this initial instability can be quenched or enhanced by changing the temperature of the alcohol relative to the water; the resulting thermal convection then opposes or reinforces the unstable motion. Similar behaviors have been well characterized in surfactant systems,^{9–18} where the corresponding instability evolves more slowly.

Surface tension gradients are responsible for the rapid motion of small alcohol lenses, as well as fingering instabilities along the lens perimeters. We show examples of fingering in 1-butanol and 3-octanol. Surface tension gradients also drive convection in the underlying water (the Marangoni effect). Convection delivers relatively pure, high-surface-tension water to the surface, complicating the local pattern of surface tension gradients. These gradients dramatically accelerate dissolution. We show that the time required for 10 μL alcohol drops to dissolve is increased by treatments that lower the solubility of alcohol in the water bath (e.g., by adding salt to the water) and by treatments that limit the surface area available for alcohol diffusion.

Although the complex behavior of liquid alcohol drops on water defies comprehensive accounting, the phenomena driving these motions are relatively simple. A more thorough understanding of these phenomena may allow for improved processes involving the interaction of fluids with limited mutual solubility. Surface tension effects can be especially important on small length scales, including those encountered in microfluidic and nanoscale devices.

Experiment

Deionized water was used throughout the experiments. The alcohols were obtained from Aldrich at a minimum purity of 97% and are primary alcohols unless otherwise noted. Synthetic DL-camphor was obtained from J.T.Baker. To visualize the alcohol lenses, resublimed iodine (Mallinckrodt) was added to the alcohol. Where noted, rhodamine 6G (LC 5900, Lambda Physik) was used in place of iodine. Experiments with undyed alcohol showed that lens behaviors were not noticeably altered by the addition of these dyes.

In most experiments, a polystyrene dish of diameter 5.3 cm was filled with 19 mL of water at room temperature ($\sim 20^\circ\text{C}$). A 10 μL alcohol drop at room temperature was then gently applied to the

* To whom correspondence should be addressed. E-mail: jtd@wsu.edu.

- (1) Darling, C. R. *Proc. Phys. Soc. London* **1912**, 24, 228–229.
- (2) Hardy, W. B. *Proc. R. Soc. London, Ser. A* **1913**, 88, 313–333.
- (3) Ramdas, L. A. *Indian J. Phys.* **1926**, 1, 1–34.
- (4) Ramdas, L. A.; Vaidyanathan, P. S. *Proc. Indian Acad. Sci.* **1938**, 7, 186–195.
- (5) Ramdas, L. A. *Indian J. Pure Appl. Phys.* **1971**, 9, 1004–1007.
- (6) Rayleigh, L. *Proc. R. Soc. London* **1890**, 47, 364–367.
- (7) Pockels, A. *Nature* **1891**, 43, 437–439.
- (8) Adamson, A. W. *Physical Chemistry of Surfaces*, 5th ed.; John Wiley: New York, 1990.
- (9) Wyart, F. B. *Langmuir* **1993**, 9, 3682–3690.
- (10) Redon, C.; Brochard-Wyart, F.; Rondelez, F. *Phys. Rev. Lett.* **1991**, 66, 715–718.
- (11) Mendes-Tatsis, M. A.; Agble, D. J. *Non-Equilib. Thermodyn.* **2000**, 25, 239–249.

- (12) Agble, D.; Mendes-Tatsis, M. A. *Int. J. Heat Mass Transfer* **2001**, 44, 1439–1449.
- (13) Kogi, O.; Yuya, K.; Kim, H.-B.; Kitamura, N. *Langmuir* **2001**, 17, 7456–7458.
- (14) Kovalchuk, N. M.; Vollhardt, D. J. *Phys. Chem. B* **2001**, 105, 4709–4714.
- (15) Afsar-Siddiqui, A. B.; Luckham, P. F.; Matar, O. K. *Adv. Colloid Interface Sci.* **2003**, 106, 183–236.
- (16) Gokhale, S. J.; Plawsky, J. L.; Wayner, P. C. J. *Langmuir* **2005**, 21, 8188–8197.
- (17) Kovalchuk, N. M.; Vollhardt, D. *Adv. Colloid Interface Sci.* **2006**, 120, 1–31.
- (18) Stocker, R.; Bush, J. W. M. *J. Fluid Mech.* **2007**, 583, 465–475.

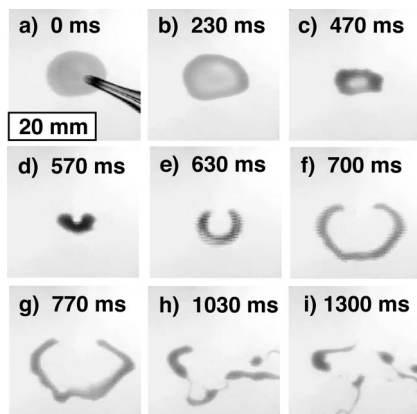


Figure 1. Fragmentation of a 10 μL drop of 1-hexanol on water. Time $t = 0$ corresponds to the acquisition of image a, just after the drop touched the surface; the pipet tip in (a) is already raised well above the drop. After initial spreading, the interior of the drop grows thin (b). The resulting lens is unstable, first collapsing (c, d) and then rebounding to form an expanding crescent (e, f). Fragmentation of the crescent produces filament-like lenses that rapidly dissolve (h, i). This produces patches of low surface tension that repel nearby lenses.

water surface. The water and/or alcohol temperature, drop volume, and container geometry were varied. The dishes were open to the air, but air currents were blocked with a shield. As the alcohols used have low volatility, the effects of evaporation were minimal. For instance, 10 μL of butanol (bp 117 $^{\circ}\text{C}$) requires about 10 min to evaporate from a watch glass under conditions similar to those in the experiments. The same volume of butanol on a water surface completely dissolved in 2–3 s. No obvious differences in drop behavior were observed in covered dishes.

The motion of alcohol lenses was imaged with a JAI CV-730 video camera mounted above the water-filled dish and recorded at 30 frames/s using InterVideo WinDVR 3 software with a resolution of 710×480 pixels. Selected video recordings have been posted on the Web for the convenience of the reader¹⁹ and provide significant insight into the effects described below.

To image the convection currents produced in the water bath, a narrow trough was constructed by gluing two large glass microscope slides (5×7.5 cm²) together along three edges with spacer rods. A layer of dyed water was introduced along the bottom of the trough. After addition of an alcohol drop, the resulting currents were imaged from the side.

Results and Discussion

Many common features of drop breakup are visible in images of dyed 1-hexanol drops on water at room temperature. Selected video frames of a typical hexanol drop appear in Figure 1. (Readers are encouraged to view the video sequence available online.¹⁹) After the drop leaves the pipet, its diameter rapidly increases to about 10 mm (Figure 1a). This radius corresponds to an average thickness of about 100 μm . Initially, the 1-hexanol “wets” the water bath, consistent with the low surface tension of pure alcohol and the high surface tension of pure water. The energy per unit area associated with this spreading is given by the spreading coefficient, S ⁸

$$S = \gamma_w - \gamma_a - \gamma_{aw} \quad (1)$$

where γ_w is the surface tension of water, γ_a is the surface tension of the alcohol, and γ_{aw} is the tension of the alcohol–water interface. For a 1-heptanol, which is representative of the 1-alcohols, $\gamma_a = 27.0$ mJ/m², for pure water, $\gamma_w = 72.8$ mJ/m²,

and for the water–heptanol interface, $\gamma_{aw} = 8.0$ mJ/m².^{8,20} The initial spreading coefficient is high, almost 38 mJ/m², and strongly favors spreading.

Because of the large surface tension of pure water, the water–air–alcohol triple point is unstable in the absence of other forces ($\gamma_w > \gamma_a + \gamma_{aw}$). For drops that exceed a critical thickness, T_c , equilibrium is attained due to the operation of gravitational forces; T_c is given by^{8,9}

$$T_c = \left[\frac{2S\rho_w}{g\rho_a(\rho_w - \rho_a)} \right]^{1/2} \quad (2)$$

where ρ_w and ρ_a are the densities of water and alcohol, respectively, and g is the acceleration of gravity. For 1-hexanol on water, $T_c \approx 2$ mm. The drop volume employed above (10 μL) is too small for the formation of such a thick lens.

As the alcohol dissolves, the surface tension of the surrounding water falls. In the limit of saturation, $\gamma_w = 28$ mN/m. This is sufficient to change the sign of the spreading coefficient, and the liquid retracts to form a compact lens. The resulting dewetting transition is marked by a rapid reduction in lens area and a rapid increase in lens thickness. Stability analysis indicates that metastable lenses thinner than T_c typically dewet by the nucleation and growth of holes, followed by the thickening of the resulting rim.⁹ The corresponding event in Figure 1 is the formation of a light-colored region inside the lens and a darkening along the rim in Figure 1b. Similar instabilities are observed when a layer of benzene is added to a water surface in an overfull crystallizing dish.²⁰ (Overfilling the crystallizing dish, so that the water surface lies slightly above the rim, ensures that the hole is nucleated in the middle of the dish and not along the edge.) A similar dewetting instability is responsible for the growth of holes nucleated in spin-coated poly(dimethylsiloxane) (PDMS) films of comparable thicknesses on fluorocarbon-coated silicon wafers.¹⁰

The thin central region in the lens of Figure 1b renders it unstable to collapse. Parts c and d of Figure 1 show this collapse on time scales of hundreds of milliseconds. Interestingly, the central region retains its light color until collapse is almost complete. Asymmetries in the initial drop shape and environment are reflected in the asymmetry of the collapse: the upper rim in Figure 1c has a particularly high downward velocity (in the plane of the image), which carries it through the center of the original lens to form a crescent or boomerang shape, open toward the top. The crescent then expands rapidly to a diameter slightly greater than that of the original lens, as shown in Figure 1e–g.

As the expansion of the crescent-shaped lens in Figure 1g slows, instabilities develop along its length and the crescent pinches off into several fragments, which then contract to form more compact lenses. As the fragments separate, they leave behind an alcohol film that dewets to form short-lived, filamentary lenses that join the separating segments. These filaments are highly unstable and dissolve rapidly to produce patches of low-surface-tension water. Nearby lenses can be repelled from these patches for many tens of milliseconds. When upwelling currents produce patches of relatively pure, high-surface-tension material, the pattern of surface tension gradients and lens motions becomes exceedingly complex.

Convection. When a drop of alcohol touches the water surface, alcohol diffuses radially outward from the perimeter of the lens (the water–air–alcohol triple point) along the water surface.^{5,21} The variation in alcohol concentration with distance from the drop produces surface tension gradients that drive radial currents

(20) Harkins, W. D. *J. Chem. Phys.* **1941**, 9, 552–568.

(21) Nagai, K.; Sumino, Y.; Kitahata, H.; Yoshikawa, K. *Phys. Rev. E* **2005**, 71, No. 065301, 1–4.

(19) URL for supporting video files: <http://honors.physics.wsu.edu/videos/videos.html>.

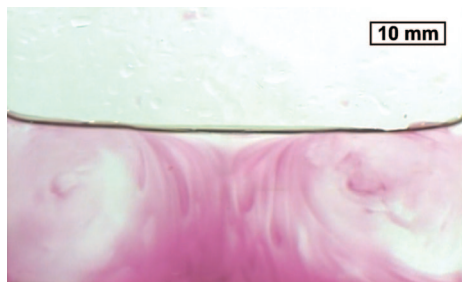


Figure 2. Side view of the narrow trough containing clear and dyed water. A drop of 1-butanol was placed on the water surface in the center of the trough. The resulting surface tension gradients drive near-surface currents that produce convection spirals on each side.

along the surface and in the underlying water (the Marangoni effect).²² The currents generated by convection can be visualized by introducing a layer of dyed water along the bottom of a narrow rectangular trough and viewing the trough from the side. Figure 2 shows an image of the dye after a drop of butanol was placed on the water surface, near the center of the trough.¹⁹ Convection rolls quickly form at each end of the trough, reflecting surface flow from the drop toward the two ends of the trough. (Readers are encouraged to view the video sequence available online.¹⁹) The velocity of the resulting currents decreases with chain length for the 1-alcohols. Nevertheless, even the longest alcohols employed in this work ($n = 9, 10$) generate visible currents. This convection dramatically accelerates dissolution by preventing the formation of a saturated alcohol–water surface layer.

The strongest currents develop along the surface just outside the lens perimeter. This is evident in the video associated with Figure 2,¹⁹ where water upwelling from below is initially directed toward the perimeter (and not the center) of the lens. As the fluid approaches the surface from below, the flow accelerates and constricts. (The cross section of an accelerating flow decreases due to conservation of mass.) As the lens shrinks, the upwelling currents become more collimated vertically. Eventually the lens dissolves entirely, and upwelling water reaches the surface near the center of the trough. For the lighter alcohols, the direction of the surface current reverses immediately after the lens disappears—presumably due to the relatively high surface tension of upwelling water near the center. Similar effects in controlled geometries produce oscillating, surface-tension-driven currents.^{23,24}

Temperature. Lens evolution can be dramatically modified by varying the temperature of the alcohol drop and the water bath. Figure 3 shows images of 1-heptanol lenses on water acquired 0.5 s after placement at the indicated alcohol and water temperatures. When the alcohol and water are both at room temperature, the 1-heptanol drop spreads to a diameter of about 10 mm in 0.5 s. However, when the water temperature is raised 20 °C or the alcohol temperature is lowered 20 °C, the drop diameter is less than 5 mm. Conversely, when the water temperature is cooled 20 °C or the alcohol is heated 20 °C, spreading is enhanced and the ringlike lens is enlarged.

In Figure 3, when the alcohol is colder than the water, the lenses remain small and initially show little activity. The evolution of a 1-heptanol lens (colored with rhodamine 6G) at an initial temperature of 1 °C on room-temperature water is shown in Figure 4. This lens retains its oval perimeter for more than a

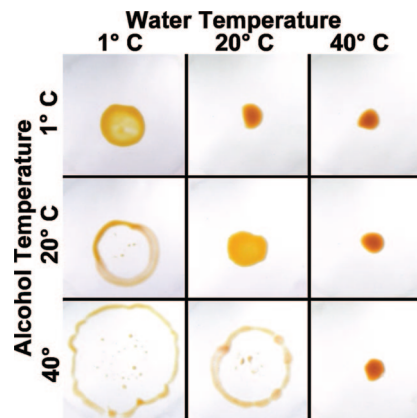


Figure 3. Drops (10 μ L) of 1-heptanol on 19 mL of water at the indicated initial alcohol and water temperatures. Each image was acquired 0.5 s after the drop touched the water.

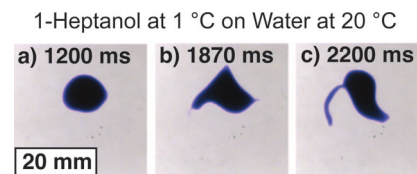


Figure 4. Initial fragmentation of a drop of 1 °C 1-heptanol on a dish containing 19 mL of 20 °C water. The images were acquired (a) 1200 ms, (b) 1870 ms, and (c) 2200 ms after the alcohol drop touched the water. To render the lens visible, rhodamine 6G was added to the alcohol.

second after placement. It then develops angular corners (Figure 4b) and fragments after local instabilities (probably vortices) draw out thin filaments (Figure 4c). In Figure 4, each corner is the source of an alcohol finger, but only the finger on the left is prominent. After this finger pinches off from the main lens, it fragments much like the crescent-shaped, 1-hexanol lens in Figure 1f.

The 20 °C temperature difference between the alcohol and the water (alcohol colder) in Figure 4 is sufficient to prevent initial spreading—despite the strongly positive spreading coefficient over this temperature range ($S > 34$ mN/m).^{25,26} We attribute the arrested spreading to thermal convection driven by density changes in the water beneath the alcohol drop.

The relative importance of gravity and surface tension in driving fluid flow can be expressed in terms of a dimensionless ratio, the Bond number, B_o

$$B_o = \frac{\Delta\rho g L^2}{\gamma} \quad (3)$$

where g is the acceleration of gravity, L is a scale length (here taken to be the dish radius, 2.6 cm), and γ is the relevant surface tension (here taken to be the spreading coefficient, about 38 mN/m). When surface tension dominates gravity, B_o is much less than 1. When gravity dominates surface tension, B_o is much greater than 1. A 20 °C drop in temperature will yield $\Delta\rho \approx 4$ mg/cm³ for water at room temperature. Under these conditions, $B_o \approx 0.7$. Thus, the effects of surface tension and gravitation are comparable and can interact in complex ways. In the present context, thermal convection hinders spreading for some seconds after lens placement. The filaments that form as these lenses

(22) O'Brien, R. N.; Feher, A. I. *J. Colloid Interface Sci.* **1975**, *51*, 366–372.

(23) Kovalchuk, N. M.; Kovalchuk, V. I.; Vollhardt, D. *Colloids Surf., A* **2002**, *198–200*, 223–230.

(24) Grigorieva, O. V.; Grigoriev, D. O.; Kovalchuk, N. M.; Vollhardt, D. *Colloids Surf., A* **2005**, *256*, 61–68.

(25) Strey, R.; Schmeling, T. *Ber. Bunsen-Ges. Phys. Chem.* **1983**, *87*, 324–327.

(26) Dilmohamud, B. A.; Seeneevassen, J.; Rughooputh, S. D. D. V.; Ramasami, P. *Eur. J. Phys.* **2005**, *26*, 1079–1084.

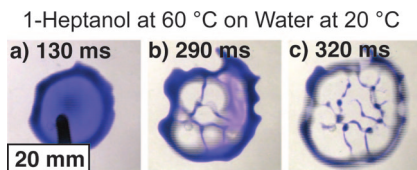


Figure 5. Images of a drop of 60 °C 1-heptanol on a dish containing 19 mL of 20 °C water. The images were acquired (a) 130 ms, (b) 290 ms, and (c) 320 ms after the alcohol drop touched the water. To render the lens visible, rhodamine 6G was added to the alcohol.

break up reflect the complexity of the resulting surface-tension- and gravity-driven currents.

When the alcohol is significantly warmer than the water, thermal convection reinforces the radially outward, surface-tension-driven flow. Therefore, the hot 1-heptanol lenses in Figure 3 initially spread to greater diameters than cold ones. Although these lenses show significant thinning in the central regions, they do not normally collapse. Their rims thicken and expand continuously.

Figure 5 shows the initial evolution of a 60 °C, 1-heptanol lens on 20 °C water. A pronounced rim forms rapidly, within about 100 ms after drop placement. As the rim of the warm alcohol expands, the central region of the lens becomes transparent to the eye and develops a cell structure, shown in Figure 5b. Once formed, the walls of the cell structure rapidly fragment into droplets, shown in Figure 5c. The images in the lower left-hand corner of Figure 3 (warm 1-heptanol on colder water) were acquired after the fragmentation of similar cell structures. Cell structure formation and wall fragmentation are consistent with the dewetting of a submicrometer-thick film.⁹ Similar instabilities have been inferred from images of polymer structures on rigid substrates acquired well after structure formation.²⁷ To our knowledge, images of the transition from a well-developed cell structure to patterned droplets during liquid–liquid dewetting have not been previously published.

Edge Instabilities and Fingering. The shortest alcohols employed in this work ($n = 4, 5$) are prone to fingering instabilities. Soon after placement on the water, lenses of 1-butanol and 1-pentanol develop fingers or protrusions that grow outward from the lens. Fingering occurs when the energy gained as a protrusion extends onto high-surface-tension water is sufficient to produce the required increase in the lens perimeter.²¹ The observed finger spacing typically corresponds to the wavelength of the fastest growing vibrational mode of the lens. For 10 μ L drops of the lighter alcohols, the wavelength of the fastest growing mode is well below the drop diameter, and many fingers are observed.

Lenses of 1-butanol and 1-pentanol on room-temperature water usually finger in a chaotic, irregular fashion. More regular patterns can appear when the alcohol is cooled and the water heated. As noted above, the radially inward convection that results tends to stabilize these lenses. Figure 6 shows a lens of cold (1 °C) butanol on hot (40 °C) water. Fingers grow outward from the butanol lens and fragment, ejecting rings of droplets.¹⁹ The central lens then contracts to re-form a circular disk, and the cycle of fingering and fragmentation repeats—often several times at roughly 200 ms intervals. “Surface jets” similar to those in Figure 6 were conjectured, but not directly observed, in a study of water/ethanol mixing.²⁸ Drops of isobutanol under water have also been observed to eject smaller drops.¹¹ Radial oscillations have also been observed in surfactant-laden drops of oil on water.¹⁸

Lenses of longer 1-alcohols ($n = 5–8$) on room-temperature water tend to elongate into crescents that quickly fragment.

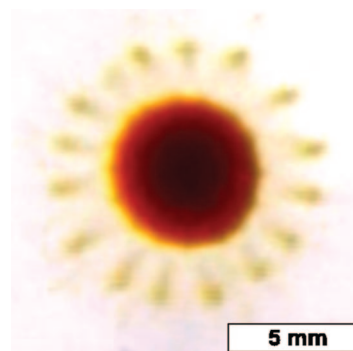


Figure 6. Drop of 1-butanol cooled to 1 °C and applied to 40 °C water. The drop pulsed several times, throwing off a ring of smaller drops each time, before random motions appeared.

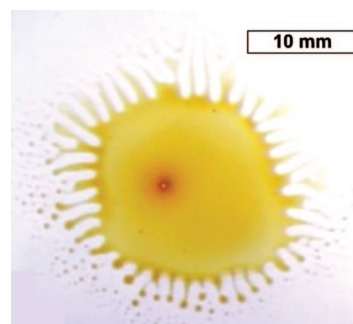


Figure 7. Drop of 3-octanol on water, both at room temperature. This alcohol showed more dramatic edge fingering than the other alcohols in this study.

Although other factors come into play, fingering instabilities involving the entire lens can develop when the wavelength of the fastest growing instability is comparable to the lens diameter.²¹ Instabilities with shorter wavelengths can appear in lenses of these longer alcohols when the alcohol group is located near the center of the carbon backbone. An image of a 3-octanol lens on room-temperature water appears in Figure 7. Irregular fingers appear soon after placement. However, subsequent finger growth is often overshadowed by the growth of voids back toward the central lens. Void growth is accompanied by fingering darkening, where alcohol is drawn into the fingers from the voids on each side. Pairs of voids coalesce at intervals, halving the number of fingers and further increasing the finger thickness and darkness. The relatively ordered pattern of fingers in Figure 7 appeared after two cycles of void coalescence. Finger fragmentation also has produced small lenses that shoot away from the main lens. A video of fingering in a 3-octanol lens has been posted on the web.¹⁹

The position of the alcohol group in 3-octanol has important effects on its interaction with water. For instance, the two chain fragments on either side of the OH group in 3-octanol both interact strongly with the alcohol phase. Thus, 3-octanol along a water–alcohol interface occupies more area per molecule than 1-octanol.²⁹ That said, a more complete accounting of alcohol properties is necessary to account for the observed behavior of 3-octanol lenses. Void growth, for instance, may reflect localized dewetting.

In contrast, 10 μ L lenses of 1-nonanol on room-temperature water are relatively inert and do not finger. They adopt a spherical shape and drift slowly across the water surface. These drops are

(27) Reiter, G. *Langmuir* **1993**, 9, 1344–1351.

(28) Walters, D. A. *Langmuir* **1990**, 6, 991–994.

(29) Chavepeyer, G.; Salajan, M.; Platten, J. K.; Smet, P. J. *Colloid Interface Sci.* **1995**, 174, 112–116.

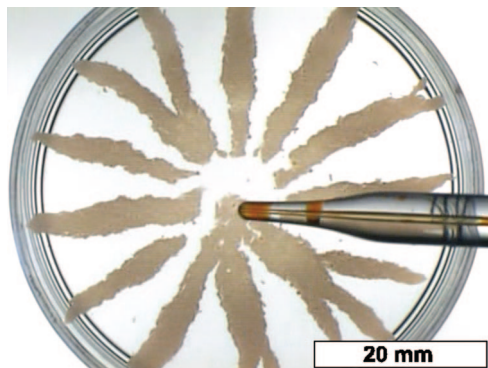


Figure 8. Drop of dodecanol (mp +24 °C) warmed to 40 °C and applied to 1 °C water. This image was acquired 0.13 s after the drop touched the water. No subsequent changes are observed.

presumably smaller than any of the associated unstable vibrational modes, and fingering is strongly hindered.

Higher Alcohols. Undecanol and dodecanol are solids at room temperature. Nevertheless, both alcohols form lenses on water when melted. Lenses of these alcohols were formed by heating the alcohol to 40 °C and then adding a 10 μ L drop to cold water (1 °C). Undecanol ($n = 11$) spreads rapidly into a large circular patch, which then solidifies. In contrast, dodecanol ($n = 12$) forms a star-shaped patch on the water surface, as shown in Figure 8.¹⁹ Dodecanol films freeze quickly and fracture, with each piece drawing out a trail, while undecanol remains liquid long enough to form a complete circle before freezing.

Lens Propulsion. Still photos can hardly convey the erratic motion of drops across the water surface. This motion is driven by surface tension gradients, where the net force on a lens is in the direction of increasing surface tension. Small drops, with their low mass-to-perimeter ratios, are accelerated most strongly. Once accelerated, small drops can move in straight lines for some centimeters and rebound ballistically from the edge of the dish.

Each lens is a local source of low-surface-tension water due to the radial, outward diffusion of alcohol. As one lens approaches another, the relatively low surface tension of the water between them allows for what appears to be a repulsive force between lenses. (In reality, the relatively high surface tension of the water on the opposite sides of the lenses draws them apart.) Lens coalescence is rare. The apparent repulsion contrasts with the commonly observed attraction between floating objects of similar size and shape (the “Cheerios effect”).³⁰

Lens repulsion is clearly demonstrated by using octadecyltrichlorosilane-treated glass rods to move two lenses together. Octanol and nonanol in particular wet octadecyltrichlorosilane well, and lenses of these alcohols can be manipulated by touching treated rods near the center of each lens. Manipulation is most effective on alcohol–water solutions. With some skill, two lenses can be forced to merge. Otherwise, the lenses slide past each other.

Role of Alcohol Solubility. The importance of alcohol solubility can be demonstrated by adding salt to the water bath. This treatment lowers the solubility of many organic compounds in water,^{31–34} but has relatively small effects on the surface tension

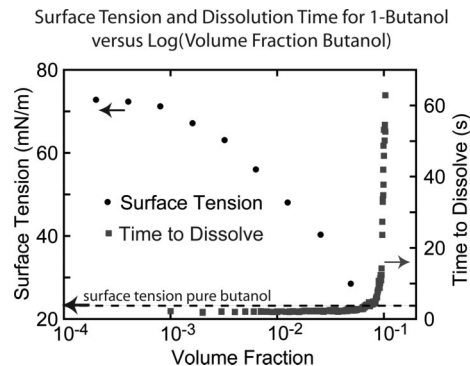


Figure 9. Surface tension and dissolution time for 10 μ L aliquots of 1-butanol during the addition of a series of aliquots. The surface tension data were taken from measurements on 1-butanol by King.³⁶

of the water phase. For instance, the solubility of 1-hexanol is 14 times lower in 5 M NaCl solution than in pure water.³⁵ In contrast, the surface tensions of saturated salt solutions are typically about 80 dyn/cm, versus 72.8 dyn/cm for pure water. We find that 10 μ L aliquots of 1-butanol drops take about 50% longer to dissolve on the surface of 5 M NaCl solutions than on nominally pure water. When the initial alcohol solubility is lower, the effect of salt is much greater: 10 μ L drops of 1-heptanol on 5 M NaCl solutions take 35 times longer to dissolve than on pure water. In these two cases, the dissolution time correlates far better with changes in alcohol solubility than with changes in surface tension.

As discussed below, alcohol solubility plays an important role in establishing the concentration gradients that enhance dissolution. The high solubility of the short-chain alcohols allows for modest surface tension gradients even at relatively high alcohol concentrations. In Figure 9, we compare the surface tension of butanol/water mixtures (from ref 36) with the time required to dissolve 10 μ L aliquots of butanol. Each aliquot was allowed to completely dissolve before the next was added. Care was taken to ensure that the dish diameter was sufficient to avoid dish size effects (discussed below)—at least at the beginning of the experiment. The horizontal axis indicates the volume fraction of alcohol in the water due to previously dissolved aliquots. The volume fraction is plotted on a logarithmic scale to emphasize the small changes in surface tension at the higher alcohol concentrations. The dissolution time for 10 μ L aliquots of 1-butanol is nearly constant until the surface tension of the mixture approaches the surface tension of pure butanol. Further increases in butanol concentration dramatically increase the dissolution time. Small surface tension gradients are apparently sufficient to cause rapid dissolution in butanol, but even these small differences disappear as the solution approaches saturation.

As the alcohol chain length increases, the dissolution time is more strongly affected by the alcohol concentration—even at concentrations well below the solubility limit. Measurements of dissolution time for successive 10 μ L aliquots are shown for 1-butanol, 1-pentanol, 1-hexanol, and 1-heptanol as a function of the alcohol concentration (here reported as a percentage of the solubility) in Figure 10. Again, each aliquot was completely dissolved before the next aliquot was added. The data for 1-butanol are taken from Figure 9. For 1-butanol, the dissolution time is almost independent of concentration until the concentration reaches 80% of the solubility limit. For 1-pentanol and 1-hexanol,

(30) Vella, D.; Mahadevan, L. *Am. J. Phys.* **2005**, *73*, 817–825.

(31) Sinegubova, S. I.; Il'in, K. K.; Cherkasov, D. G.; Kurskii, V. F.; Tkachenko, N. V. *Russ. J. Appl. Chem.* **2004**, *77*, 1924–1928.

(32) Malinowski, J. J.; Daugulis, A. J. *AIChE J.* **1994**, *40*, 1459–1465.

(33) Reber, L. A.; McNabb, W. M.; Lucasse, W. W. *J. Phys. Chem.* **1942**, *46*, 500–515.

(34) Feldkamp, D.-I. K. *Chem.-Ing.-Tech.* **1968**, *40*.

(35) Ni, N.; El-Sayed, M. M.; Sanghvi, T.; Yalkowsky, S. H. *J. Pharm. Sci.* **2000**, *89*, 1620–1625.

(36) King, H. H. *Adsorption at Liquid-Vapor and Liquid-Liquid Interfaces and Some Related Phenomena*; Kansas State Printing Plant: Topeka, KS, 1922.

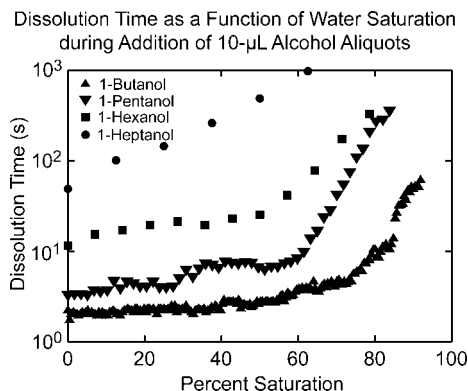


Figure 10. Dissolution time for 10 μL aliquots of alcohol dissolving on 19 mL of water. The indicated level of saturation refers to the alcohol concentration before each aliquot is added.

the dissolution time gradually increases with concentration at low concentrations and rises sharply as the alcohol concentration reaches 50–60% of the solubility limit. The dissolution time for 1-heptanol increases steadily with alcohol concentration, even at the lowest concentrations tested.

The surface tension gradients that drive convection reflect alcohol concentration gradients along the surface. To demonstrate how these concentration gradients depend on solubility, we present a simple model from Nagai et al.²¹ for the radial diffusion of alcohol along the surface from a circular alcohol lens. The diffusion rate is given by the product of a surface diffusion constant D and the radial surface concentration gradient, dc/dr . As alcohol diffuses radially along the surface, it also dissolves in the underlying water. The rate of alcohol dissolution is proportional to the difference between the alcohol solubility in the bulk, c_{max} , and the actual alcohol concentration in the underlying water, c_a . (Prior to dissolution, $c_a = 0$.) In this simple model, we neglect evaporation and convection. Under these conditions, the concentration of alcohol at the surface will vary with time as:

$$\frac{dc}{dt} = D\nabla^2 c - \alpha(c_{\text{max}} - c_a) \quad (4)$$

where α is a constant that reflects the dissolution rate. We further assume that the flux of alcohol from the perimeter of the lens is proportional to the alcohol activity at the perimeter (assumed to be unity) and yields a constant flux per unit perimeter length.^{4,37,38} The steady-state solutions to eq 3 in the limit of large dishes yield concentration gradients, evaluated at the perimeter of the drop, of the form

$$\frac{dc}{dr} = (c_{\text{max}} - c_a) \left(\sqrt{\frac{\alpha}{D}} \right) \frac{K_1 \left(\sqrt{\frac{\alpha}{D}} R \right)}{K_0 \left(\sqrt{\frac{\alpha}{D}} R \right)} \quad (5)$$

where R is the lens radius and K_0 and K_1 are zero- and first-order modified Bessel functions.

In the early stages of dissolution, $c_{\text{max}} \gg c_a$, and the surface tension gradient at the lens perimeter is proportional to the solubility. The variation in alcohol solubility with chain length is therefore an extremely important factor in the stability and lifetime of alcohol lenses. The dissolution rate constant α and the diffusion constant D appear only in the ratio α/D , which

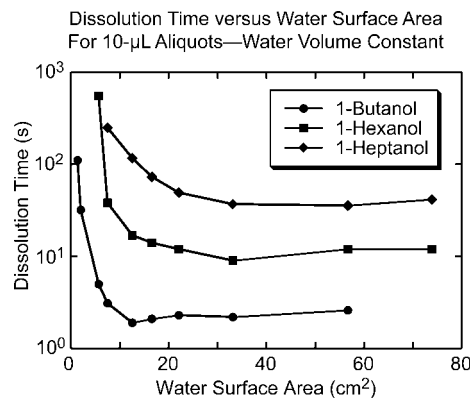


Figure 11. Time required for 10 μL aliquots of 1-butanol, 1-hexanol, and 1-heptanol to completely dissolve into 19 mL of water as a function of the water surface area. Each 10 μL drop was allowed to dissolve completely before the next was added.

defines a scale distance for the change in concentration gradient with lens radius. This same scale distance applies to the change in alcohol concentration with distance away from the lens. As both α and D tend to decrease with the alcohol chain length, this scale distance is probably a weak function of the chain length. The ratio of the modified Bessel functions diverges at low R (the small-lens limit) and asymmetrically approaches unity for large R . Thus, the concentration gradients are especially great along the perimeter of small lenses.

Effect of Dish Area. Solutions of eq 3 imply that the surface alcohol concentration around an ideal, circular lens drops to zero at a finite distance from the lens. The limited spread of dyed alcohol in a water-filled dish can often be observed visually. For instance, the film surrounding a 10 μL volume of heptanol in a sufficiently large dish of room-temperature water occupies an average maximum area of about 27 cm^2 , even after lens fragmentation. Constraining the area available for spreading to lower values can have dramatic effects on the dissolution time.

Figure 11 shows the time required to completely dissolve 10 μL lenses as a function of the container diameter for three alcohols. The total volume of water was the same for each trial. As long as the dish area exceeds the maximum spreading area, the dissolution time is almost independent of the dish area and increases with the alcohol chain length. The dissolution time for 10 μL drops of 1-heptanol, for instance, is nearly constant for areas greater than 25 cm^2 . As the dish diameter drops below this maximum, the dissolution time increases dramatically. We attribute the bulk of this increase to the suppression of surface tension gradients as the alcohol-rich water begins to cover the entire water surface. In the absence of surface-tension-driven flow (the Marangoni effect), dissolution takes much longer.

The alcohol from large drops will spread over larger areas than the alcohol from small drops. If this area exceeds the dish area, dissolution slows dramatically. For instance, 1 mL of 1-butanol on 19 mL of water in a 5.3 cm diameter Petri dish takes about 1 h to dissolve, and the resulting solution is highly stratified. When the same amount of alcohol is added to the dish in small aliquots, so that the butanol surface film never completely covers the water surface, the entire volume can be added in less than 3 min; the resulting solution appears to be well-mixed.

Figure 12 shows the time required for room-temperature 1-heptanol drops to dissolve as a function of the drop volume for dishes with four different surface areas. Each container holds the same volume of water, which was chosen to keep the heptanol concentration well below the solubility limit after the largest drops dissolve. In the largest dishes, the apparent dissolution

(37) Suciu, D. G.; Smigelschi, O.; Ruckenstein, E. *AIChE J.* **1967**, *13*, 1120–1124.

(38) Nakata, S.; Iguchi, Y.; Ose, S.; Kuboyama, M.; Ishii, T.; Yoshikawa, K. *Langmuir* **1997**, *13*, 4454–4458.

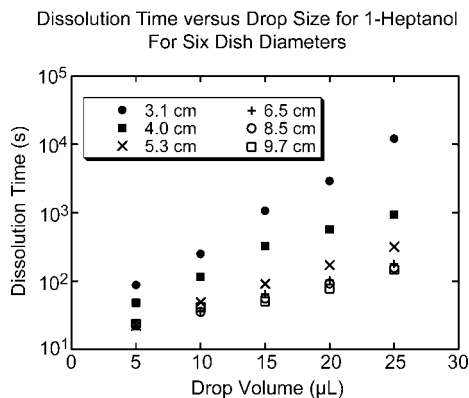


Figure 12. Dissolution times for drops of 1-heptanol on 19 mL of water as a function of the drop size for dishes of six different diameters. The standard deviations of the measurements (not shown) are about the size of the plotted symbols.

time for each drop size is almost independent of the dish size. In the smallest dishes (3.1, 4.0, and 5.3 cm in diameter), the dissolution times increase more rapidly with drop size. The surface areas of these dishes are less than the 27 cm² required to accommodate the film around a 10 μL heptanol lens; the other dishes are larger.

Figure 12 shows that increasing the dish diameter beyond 6.5 cm (area 33 cm²) has little effect on the dissolution time, even for the largest drops employed. This suggests that the effective area of the spreading film is a weak function of the drop volume. This is consistent with the simple model of eqs 3 and 4. For $(\alpha/D)^{1/2}R \gtrsim 1$, the predicted spreading area varies approximately with the cube root of the drop volume. Therefore, a large change in the drop volume is required to significantly increase the area of the spreading alcohol.

Similar experiments show that the time required for 1-heptanol to dissolve under these conditions does not depend significantly on the water depth, as long as the water volume is sufficient to keep the final solution concentration well below the solubility limit. The dish diameter-to-depth ratio does not appear to be important for the small drops employed here. Ramdas likewise found that the dissolution times for camphor did not depend on the depth of the water bath.⁴

Conclusions

The complex motion of alcohol drops on water has attracted study for over 100 years.³⁹ The transition from initial spreading behavior to nonspreading behavior is accompanied by a surprising range of phenomena, from the relatively symmetric collapse of Figure 1 (1-hexanol) to finger formation in Figure 7 (3-octanol). As dissolution proceeds, surface tension gradients propel and often fragment alcohol lenses, dramatically accelerating dissolution. Of particular interest are the filament-like lenses that form between separating lens fragments and void fingers. The unstable dissolution of these filaments can yield especially large, local reductions in surface tension with dramatic effects on nearby lenses.

Short-chain alcohols ($n \leq 5$) are highly soluble in water. Small drops on pure water fragment quickly due to dewetting instabilities and surface tension gradients. These effects dramatically accelerate dissolution. Long-chain alcohols ($n > 8$) are much less soluble in water, and the resulting surface tension gradients are weak. Lenses of these alcohols appear inert, and dissolution is slow. In the intermediate range of chain lengths ($n = 6-8$), the cohesive and Marangoni forces are of similar magnitude and produce especially complex behavior.

Because partial dissolution of the alcohol lens is required to generate surface tension gradients, alcohol solubility plays an important role in determining lens behavior. Treatments that decrease the alcohol solubility have dramatic effects on the observed dissolution rates. For example, adding salt to the water increases the local surface tension but decreases the alcohol solubility: the net effect is to slow the dissolution of alcohol drops. By understanding the interaction of surface tension and solubility, these effects can be exploited more effectively in applications such as mixing, extraction, and microfluidics.

Acknowledgment. This work was supported by the National Science Foundation under Grant CMS-04-09861, an associated REU, and the Department of Energy under Grant DE-FG02-04ER-15618.

LA800105H

(39) Thomson, J. *London, Edinburgh Dublin Philos. Mag. J. Sci.* **1855**, 10, 330–333.